

Right-handed neutrino pair production via second-generation leptoquarks

Arvind Bhaskar,^{1,*} Yash Chaurasia,^{1,†} Kuldeep Deka,^{2,‡} Tanumoy Mandal,^{3,§} Subhadip Mitra,^{1,¶} and Ananya Mukherjee^{4,**}

¹Center for Computational Natural Sciences and Bioinformatics,
International Institute of Information Technology, Hyderabad 500 032, India

²Department of Physics and Astrophysics, University of Delhi, Delhi 110 007, India

³Indian Institute of Science Education and Research Thiruvananthapuram, Vithura, Kerala, 695 551, India

⁴Theory Division, Saha Institute of Nuclear Physics, 1/AF Bidhannagar, Kolkata 700 064, India

There are no direct experimental constraints on the Leptoquark (LQ) couplings with quarks and right-handed neutrinos (RHNs). If a (scalar or vector) LQ dominantly couples to RHNs, it can leave unique signatures at the LHC. The RHNs can be produced copiously from LQ decays as long as they are lighter than the LQs. The LQ-induced RHN production mechanism has never been searched for in experiments. This channel can act as a simultaneous probe for both RHNs and LQs that dominantly couple to RHNs. In this paper, we consider all possible charge-2/3 and 1/3 scalar and vector LQs that exclusively couple to a second-generation quark and a RHN. We study the pair and single productions of TeV-scale LQs and their subsequent decay to sub-TeV RHNs, realised in the inverse seesaw framework. The single production contribution can be significant for large LQ-RHN-quark couplings. We systematically combine the pair and single production events leading to a pair of RHNs plus jets to study the prospects of this channel. We analyse the monolepton and opposite-sign dilepton final states and estimate the discovery reach at the high-luminosity LHC.

I. INTRODUCTION

The neutrino oscillation data provide vital evidence for the presence of physics beyond the Standard Model (SM) by pointing towards the neutrino masses. However, probing the neutrino sector at particle colliders is not simple. Due to their elusive nature, the light neutrinos pass through the detectors undetected. Generally, one considers heavy right-handed neutrinos (RHNs, ν_R 's) to generate light-neutrino masses through the seesaw mechanism. In principle, the LHC could probe RHNs if they are within the TeV scale. Observing RHNs at the LHC would be an important milestone since, apart from the neutrino mass generation mechanism, they have the potential to shed light on other serious issues like dark matter, matter-antimatter asymmetry, etc. However, a straightforward application of the vanilla seesaw mechanism (Type-I) [1, 2] puts the RHNs several orders of magnitude above the TeV scale. But, there are other possible ways to generate the masses—like the inverse seesaw mechanism (ISM) [3, 4]—where the RHNs can be within reach of the LHC.

However, even the TeV-scale RHNs are not easy to produce at the LHC (see Ref. [5] for the prospect study of RHNs at e^+e^- colliders). Since they are singlet under the SM gauge group, they interact very feebly with the SM fields through their small overlaps with the left-handed neutrinos. RHNs can be produced through the decay of another particle like W' [6, 7], Z' [8–11], etc. Since LHC is a hadron collider, RHNs can also be produced copiously through some intermediate new particle that couples with

the strong sector. In this paper, we consider an intermediary that fits naturally in this picture, namely, the leptoquark (LQ). LQs are hypothetical coloured scalar or vector bosons with both baryon and lepton numbers. As a result, they can act as connectors between the baryon and lepton sectors. They appear in various beyond-the-SM theories like Pati-Salam [12], Grand Unified Theories [13], different composite theories [14], or the R -parity-violating Supersymmetry [15], etc. Nowadays, they have become popular in the literature for explaining various experimental anomalies, like the ones seen in $R_{D^{(*)}}$, $(g-2)_\mu$, W -mass, etc. [16–19]. The phenomenology of LQs and discovery prospects for different colliders can be found in Refs. [20–25].

The LHC has an ongoing LQ search program. Both ATLAS and CMS Collaborations have looked for single and pair production of LQs in final states made of various combinations of leptons (ℓ or ν_L) and jets (light or t jet). The current mass exclusion limit on scalar (vector) LQ goes up to 1.73 [26] (1.98 [27]) TeV. There are also indirect bounds on LQ couplings (LQ-quark-lepton) from the high- p_T dilepton or monolepton + MET data [16, 18]. A LQ can simultaneously couple with a SM quark and a RHN. However, none of the direct or indirect bounds concerns this coupling. A LQ can decay to a RHN+jet final state if the RHN is lighter than the LQ. Now, if the LQ decays exclusively (or predominantly) through this mode, it becomes unrestricted by all the direct or indirect bounds. In other words, a large part of the LQ parameter space remains unrestricted by the LHC bounds.

In this paper, we utilise this freedom to study the production of RHNs via LQs at the hadron collider (similar and related phenomenological studies are found in Refs. [28–32]). If we assume the LQ couples with no other lepton except the RHNs, there are two possible production processes for the RHNs—they can come from a LQ decay, or they can be directly pair produced by a t -channel LQ exchange in the quark fusion mode. As we discuss later, the LQ-decay mode is more promising than the t -channel LQ exchange if

* arvind.bhaskar@research.iiit.ac.in

† yash.chaurasia@research.iiit.ac.in

‡ kuldeepdeka.physics@gmail.com

§ tanumoy@iisertvm.ac.in

¶ subhadip.mitra@iiit.ac.in

** ananyatezpur@gmail.com

the RHNs are lighter than the LQ. One reason is that LQs can be produced copiously through strong interaction. Secondly, the cross-section of the t -channel LQ-exchange process is susceptible to the LQ-quark-lepton coupling (goes as the fourth power); unless the coupling is of order one or larger, its cross-section is relatively smaller. Hence, in this paper, we mainly focus on the LQ-decay mode.

For our purpose, then, we consider a setup where the light neutrinos get their masses through the ISM. In the ISM, there are three extra neutral fermions (S_{L_i} with $i \in \{1, 2, 3\}$ being the generation index, all singlets under the SM gauge group) in addition to three RHNs (one for each generation). Due to the presence of these extra fermions, the RHNs can have (sub-)TeV-range masses. We consider the parameter region where the RHNs are lighter than the LQ, which decays exclusively through the RHN+jet decay mode. After production, for the LHC to detect their signatures, the RHNs should decay to SM particles within the detectors, i.e., they should not be long-lived. In our case, they decay mainly through the $\nu_R \rightarrow W^\pm \ell^\mp$ or $\nu_R \rightarrow Z/h \nu_\ell$ processes. Generally, the strongest collider bounds on the RHNs come from the searches for same-sign dilepton pairs, the signature of the Majorana nature of the RHNs. However, these bounds do not affect our analysis as the RHNs are pseudo-Dirac types in ISM.

LQs can have inter or intra-generational couplings, i.e., the quark and the lepton coupling to a LQ need not be of the same generation. The LQs that dominantly couple to third-generation fermions should be separately searched for from those coupling (mostly) to lighter generations [22, 24, 33]. This is because the detection strategies for the third-generation fermions are very different from the first two generations. There are also significant differences in the single and indirect LQ-production cross sections depending on whether they couple to the first or second-generation quarks. This happens for the obvious reason that the first-generation quarks have the largest parton distribution functions (PDFs). In this paper, we consider only second-generation interactions, i.e., we assume that a LQ exclusively decays to a second-generation quark and a RHN and, while decaying, the RHN produce a second-generation lepton in the final state. There are two reasons for this choice. First, the muon-detection efficiency is slightly better than the electron-detection at the LHC. Second, and more importantly, the second-generation case gives us a conservative estimate of the discovery/exclusion prospects of this channel. Due to the larger PDFs, the first-generation prospects are better. Moreover, the difference between the up and down quark PDFs implies, in the first-generation case, the reach of this channel would depend on the charge of the LQ producing the RHN. We shall report the prospects for the first and third-generation cases separately.

The paper is organised as follows. We make a quick review of the ISM in the next section. In Sec. III, we list the possible LQ models with RHN-decay mode and introduce some simple phenomenological models. In Sec. IV, we discuss the signals and the backgrounds and present our results in Sec. V. Finally, we conclude in Sec. VI.

II. THE INVERSE SEESAW MECHANISM

We can write the neutrino-sector interaction Lagrangian in our setup as

$$-\mathcal{L} \supset \lambda_\nu^i \bar{L}_i \tilde{H} \nu_{R_i} + M_R \bar{\nu}_{R_i}^C S_{L_i}^C + \frac{1}{2} \mu \bar{S}_{L_i} S_{L_i}^C + \text{H.c.}, \quad (1)$$

where i is the generation index, L_i is the i th lepton doublet, $\tilde{H} = i\sigma_2 H^*$, and the superscript C denotes charge conjugation. In the $(\nu_L^C \nu_R S_L^C)^T$ basis, the neutrino mass matrix can be written as

$$\mathbf{M}_\nu = \begin{pmatrix} \mathbf{0} & \mathbf{m}_D & \mathbf{0} \\ \mathbf{m}_D^T & \mathbf{0} & \mathbf{M}_R \\ \mathbf{0} & \mathbf{M}_R^T & \mu \end{pmatrix}, \quad (2)$$

where all of \mathbf{m}_D , \mathbf{M}_R and μ are 3×3 mass matrices. The light-neutrino masses are obtained after block diagonalising the mass matrix as the following,

$$\mathbf{m}_\nu = \mathbf{m}_D (\mathbf{M}_R^T)^{-1} \mu \mathbf{M}_R^{-1} \mathbf{m}_D^T. \quad (3)$$

For the heavy components, the 6×6 mass matrix in the $(\mathbf{N}_R \mathbf{S})$ basis can be written as

$$\mathbf{M}_\nu^{6 \times 6} = \begin{pmatrix} \mathbf{0} & \mathbf{M}_R \\ \mathbf{M}_R^T & \mu \end{pmatrix}, \quad (4)$$

where μ is the lepton-number violating scale that essentially acts as the source of tiny non-degeneracy among the final pseudo-Dirac pairs.

III. SCALAR AND VECTOR LEPTOQUARK MODELS

We list the LQs—scalars (sLQ) and vectors (vLQs)—with interactions with the RHNs [34]. We ignore the diquark operators to bypass the proton-decay constraints. We assume the Cabibbo-Kobayashi-Maskawa quark-mixing matrix to be diagonal for simplicity.

A. Scalar LQs

■ $\tilde{R}_2 = (\bar{\mathbf{3}}, \mathbf{2}, 1/6)$: The interaction of \tilde{R}_2 can be written as follows,

$$\mathcal{L} \supset \tilde{y}_{2ij}^{\overline{LR}} \bar{Q}_L^{i,a} \tilde{R}_2^a \nu_R^j + \text{H.c.}, \quad (5)$$

where \bar{Q}_L denotes the left-handed quark doublet, $a, b = 1, 2$ are the $SU(2)$ indices, and $\varepsilon = i\sigma^2$. The terms relevant to our analysis are

$$\mathcal{L} \supset \tilde{y}_{2ii}^{\overline{LR}} \bar{u}_L^i \nu_R^i \tilde{R}_2^{2/3} + \tilde{y}_{2ii}^{\overline{LR}} \bar{d}_L^i \nu_R^i \tilde{R}_2^{-1/3} + \text{H.c.} \quad (6)$$

■ $S_1 = (\bar{\mathbf{3}}, \mathbf{1}, 1/3)$: The only relevant term in the interaction Lagrangian of S_1 is

$$\mathcal{L} \supset -\tilde{y}_{1ii}^{\overline{RR}} \bar{d}_R^i S_1 \nu_R^i + \text{H.c.} \quad (7)$$

■ $\bar{S}_1 = (\bar{\mathbf{3}}, \mathbf{1}, -2/3)$: The relevant term is

$$\mathcal{L} \supset +\tilde{y}_{1ii}^{\overline{RR}} \bar{u}_R^i \bar{S}_1 \nu_R^i + \text{H.c.} \quad (8)$$

B. Vector LQs

■ $\tilde{V}_2 = (\bar{\mathbf{3}}, \mathbf{2}, -1/6)$: The RHN interaction of \tilde{V}_2 can be written as

$$\mathcal{L} \supset \tilde{x}_{2ij}^{\overline{LR}} \bar{Q}_L^C i^a \gamma^\mu \varepsilon^{ab} \tilde{V}_{2,\mu}^j \nu_R^i + \text{H.c.}, \quad (9)$$

which gives us the terms relevant to our analysis:

$$\mathcal{L} \supset \tilde{x}_{2ii}^{\overline{LR}} \bar{u}_L^C i \gamma^\mu \nu_R^i \tilde{V}_{2,\mu}^{-2/3} - \tilde{x}_{2ii}^{\overline{LR}} \bar{d}_L^C i \gamma^\mu \nu_R^i \tilde{V}_{2,\mu}^{-1/3} + \text{H.c.} \quad (10)$$

■ $\tilde{U}_1 = (\bar{\mathbf{3}}, \mathbf{1}, -1/3)$: The only relevant term for \tilde{U}_1 is as follows,

$$\mathcal{L} \supset \tilde{x}_{1ii}^{\overline{RR}} \bar{d}_R^i \gamma^\mu \tilde{U}_{1,\mu} \nu_R^i + \text{H.c.}, \quad (11)$$

■ $U_1 = (\bar{\mathbf{3}}, \mathbf{1}, 2/3)$: The relevant term for U_1 is as follows,

$$\mathcal{L} \supset \tilde{x}_{1ii}^{\overline{RR}} \bar{u}_R^i \gamma^\mu \tilde{U}_{1,\mu} \nu_R^i + \text{H.c.}, \quad (12)$$

C. Simple models

In the spirit of Refs. [22, 24, 33], we can express the LQ interactions generically in terms of some phenomenological Lagrangians:

$$\mathcal{L} \supset \lambda_1 \bar{d}_L \nu_R \phi_1 + \lambda_2 \bar{u}_L \nu_R \phi_2 + \text{H.c.}, \quad (13)$$

$$\mathcal{L} \supset \Lambda_1 \bar{d}_R (\gamma \cdot \chi_1) \nu_R + \Lambda_2 \bar{u}_R (\gamma \cdot \chi_2) \nu_R + \text{H.c.}, \quad (14)$$

where d and u are generic down and up-type quarks, respectively, coupling with the same-generation RHN with strength $\lambda_i (\Lambda_i)$. Since we do not consider models with more than one type of LQs in our analysis, we drop the index and refer to the couplings as $\lambda (\Lambda)$ in the rest of the paper. Moreover, we assume these couplings are real for simplicity. The kinetic terms of the vLQ Lagrangians contain an extra parameter, κ [34],

$$\mathcal{L} \supset -\frac{1}{2} \chi_{\mu\nu}^\dagger \chi^{\mu\nu} + M_\chi^2 \chi_\mu^\dagger \chi^\mu - i g_s \kappa \chi_\mu^\dagger T^a \chi_\nu G^{a\mu\nu}, \quad (15)$$

where $\chi_{\mu\nu}$ stands for the field-strength tensor of χ . The cross-section of the pair and single production of vLQs depends on κ . Here, we consider only two benchmark values, $\kappa = 0$ and $\kappa = 1$.

IV. LHC PHENOMENOLOGY

We implement the phenomenological Lagrangian terms in FEYNRULES [35] to generate UNIVERSAL FEYNRULES OUTPUT files [36] needed for MADGRAPH5 [37] to generate the signal and background events at the leading order. We use the default dynamical scale choice in MADGRAPH5 for event generation. Whenever available, we account for higher-order cross-sections with appropriate K factors. In particular, among the signal processes, we use a next-to-leading-order QCD K -factor of 1.3 for the pair production of the sLQs [38, 39]. We pass the parton-level events first

through PYTHIA8 [40] for showering and hadronisation and then through DELPHES3 [41] for detector simulation with the default CMS card. The jets are reconstructed from the DELPHES tower objects with anti- k_T clustering algorithm [42] in FASTJET [43]. We use jets of two different radii in our analysis: (a) AK4 jets with $R = 0.4$ and (b) AK8 fatjets with $R = 0.8$.

A. LQ production

At the LHC, LQs can be produced as resonances in pairs (mainly through strong interactions) or singly (mediated by the LQ-quark-RHN coupling, λ/Λ). We show the different production cross sections in Fig. 1 for $M_{\nu_R} = 500$ GeV and $\lambda = 1$ or $\Lambda = 1$ with $\kappa = 0, 1$. LQs can be produced non-resonantly through the t -channel exchange leading to pair production of RHN. We also show these cross sections along with the pair and single productions of LQs for comparison. The cross sections for the $pp \rightarrow \nu_R \nu_R$ process (t -channel LQ exchange) are smaller compared to the pair and single productions for lower LQ masses. Moreover, it is much suppressed for sLQs as compared to the vLQs. However, the $pp \rightarrow \nu_R \nu_R$ process becomes important for larger couplings as its cross section grows as λ^4 or Λ^4 . If LQs couple with the first-generation quarks, the RHN pair production cross section gets an additional boost from the larger PDFs. Both pair and single production cross sections depend on the $g\chi\chi$ coupling, κ .

As discussed earlier, the LQ-production cross sections are larger than the t -channel LQ exchange, especially for $M_{LQ} \lesssim 1.5$ GeV and order-one new coupling (λ or Λ). Since there is no direct experimental bound on the LQs decaying exclusively through RHNs, they can be even lighter than a TeV. Hence, we focus on the more promising process for better prospects. Moreover, we employ the strategy of combining different signal processes to enhance the discovery/exclusion prospects of these processes. Earlier, in Refs. [44, 45], we proposed this strategy and showed how one can systematically combine pair and single production processes leading to the same final states without double counting, and later in Refs. [22, 24, 33, 46], we demonstrated the usefulness of it.

The LQ production processes can be classified in terms of the number of charged leptons in the final state:

- (a) **Monolepton final state:** Ones with a muon accompanied by jet(s), fatjet(s) (from the hadronic decays of heavy bosons generated in the ν_R decay) and some missing E_T . The pair and single production channels contribute in the following manner:

$$pp \rightarrow \left\{ \begin{array}{l} \phi\phi/\chi\chi \\ \phi/\chi \nu_R (+j) \end{array} \right\} \rightarrow \left\{ \begin{array}{l} (j\nu_R)(j\nu_R) \\ (j\nu_R)\nu_R (+j) \end{array} \right\} \rightarrow \mu^\pm W_h^\mp Z_h \nu_L + \text{jet(s)}. \quad (16)$$

- (b) **Dilepton final state:** Ones with a opposite-sign muon pair ($\ell^+ \ell^-$) plus jet(s) and fatjet(s). The pair and single productions of LQ contribute to the dilep-

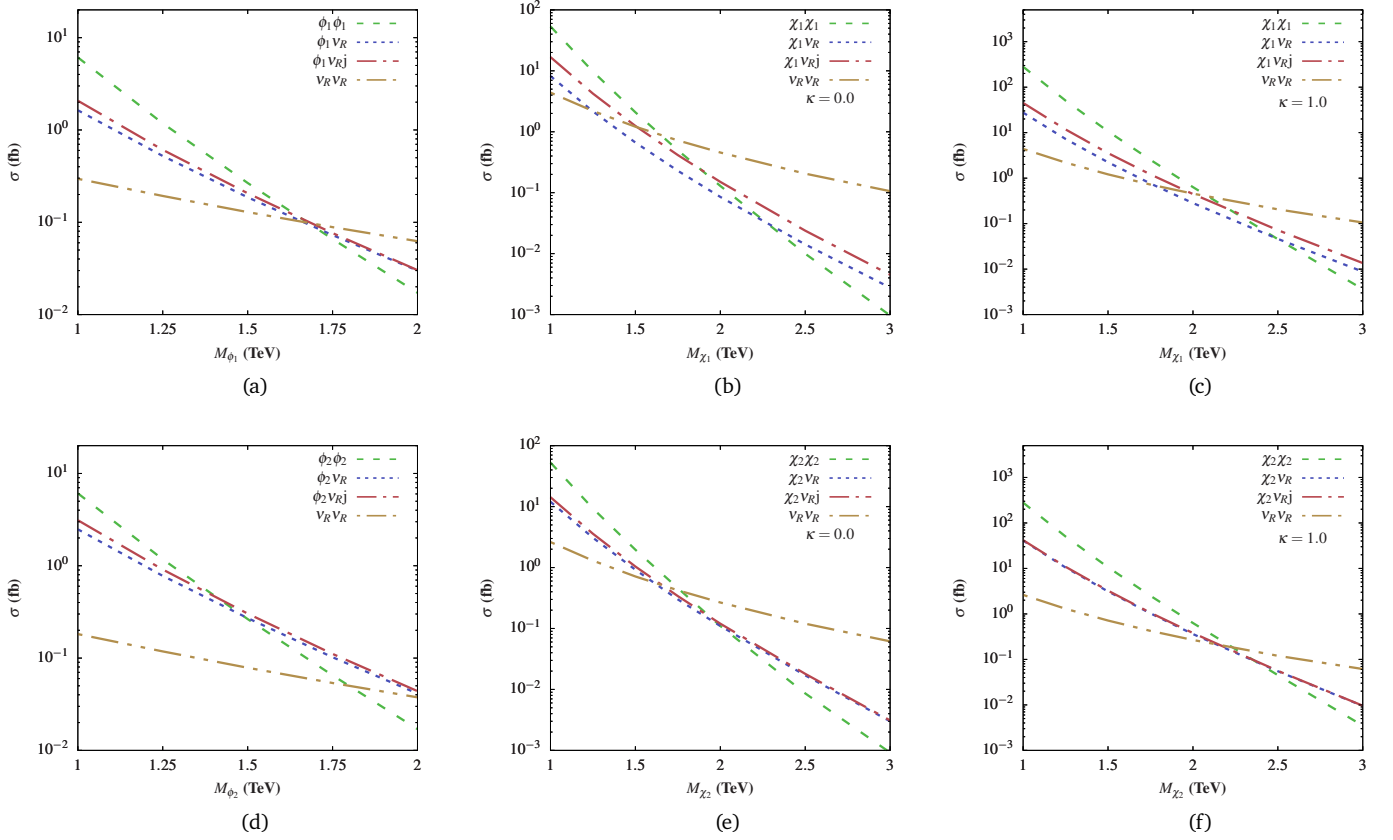


FIG. 1. Cross-sections of different production modes of sLQs [(a) and (d)] and vLQs [(b), (c), (e), and (f)]. We also show the cross-section of RHN pair production through t -channel LQ exchange. The LQ single productions and RHN pair production process are computed for $\lambda(\Lambda) = 1$. The additional $g\chi\chi$ coupling $\kappa = \{0, 1\}$.

ton final states as

$$pp \rightarrow \left\{ \begin{array}{l} \phi\phi/\chi\chi \\ \phi/\chi v_R (+j) \end{array} \right\} \rightarrow \left\{ \begin{array}{l} (jv_R)(jv_R) \\ (jv_R)v_R (+j) \end{array} \right\} \\ \rightarrow \mu^\pm \mu^\mp W_h^\pm W_h^\mp + \text{jet}(s). \quad (17)$$

In principle, one can also get more than two leptons in the final state, where the extra leptons come from the decays of the vector bosons. However, since the leptonic branchings of the heavy vector bosons are smaller than their hadronic branchings, we do not consider final states with more than two muons.

B. Signals, cuts and the background

We define our signal selection criteria to retain the inclusive mono-lepton and dilepton events:

(a) A mono-lepton event must have

- exactly one high- p_T muon and
- at least one high- p_T AK4 jet and at least one AK8 fat-jet.

(b) A dilepton event must have

Background processes		σ (pb)	QCD order
V+ jets [47, 48]	Z+ jets	6.33×10^4	NNLO
	W+ jets	1.95×10^5	NLO
	WW+ jets	124.31	NLO
VV+ jets [49]	WZ+ jets	51.82	NLO
	ZZ+ jets	17.72	NLO
	tW	83.10	N ² LO
Single t [50]	tb	248.00	N ² LO
	tj	12.35	N ² LO
	tt [51]	tt + jets	988.57
ttV [52]	ttZ	1.05	NLO+NNLL
	ttW	0.65	NLO+NNLL

TABLE I. Cross-sections of the major background processes without any cut. The higher-order cross-sections are taken from the literature; the corresponding QCD orders are shown in the last column. We use these cross-sections to compute the K factors to incorporate the higher-order effects.

- a pair of opposite-sign muons, at least one of which should have high- p_T .
- at least one high- p_T AK4 jet and at least one AK8 fat-jet.

The relevant background processes are listed in Table I.

Selection cuts	Channel	
	Monolepton	Dilepton
\mathcal{C}_1 : Selection of high p_T Leptons and jets	$p_T(\mu) > 200$ GeV, $p_T(j_1) > 200$ GeV, No b -tagged jet	$p_T(\mu) > 220$ GeV, $p_T(j_1) > 200$ GeV
\mathcal{C}_2 : Identification of fatjet	$p_T(\text{fj}) > 80$ GeV, $\tau_{21} < 0.30$, $\text{fj}_{\text{HT}} > 600$ GeV, $65 < M(\text{fj}) < 100$ GeV, $\Delta R(\text{fj}, \mu) > 1.5$	$p_T(\text{fj}_{\phi(\chi)}) > 120$ (180) GeV, $\tau_{21} < 0.30$, $\text{fj}_{\text{HT}} > 600$ GeV, $65 < M(\text{fj}) < 100$ GeV, $\Delta R(\text{fj}, \mu) > 0.8$
\mathcal{C}_3 : Lepton-fatjet invariant mass	$M(\text{fj}, \mu) > 100$ GeV	$M(\text{fj}, \mu) > 100$ GeV
\mathcal{C}_4 : Scalar cuts	$S_T > 1400$ GeV, $\cancel{E}_T > 150$ GeV	$S_T > 1400$ GeV

TABLE II. The selection cuts applied on the monolepton and dilepton final states. Here fj denotes a fatjet.

■ Monolepton final state	Selection cuts			
	\mathcal{C}_1	\mathcal{C}_2	\mathcal{C}_3	\mathcal{C}_4
Signal benchmarks				
$M_{\phi_1} = 1250$ GeV, $M_{\nu_R} = 500$ GeV (pair production)	456	183	183	150
$M_{\phi_1} = 1250$ GeV, $M_{\nu_R} = 500$ GeV (single production)	505	217	217	144
Total number of monolepton signal events:				294
Background processes				
$W_\ell (+2j)$	45259450	295099	295099	21859
$t_\ell + b/j$	3313	205	205	12
$t_\ell W_\ell (+2j)$	22349	314	314	68
$t_h t_\ell (+2j)$	168345	6943	6943	441
$W_\ell Z_\ell (+2j)$	43012	462	462	63
$t_\ell t_\ell (+2j)$	46346	801	801	121
$W_\ell W_\ell (+2j)$	34802	303	303	57
Total number of background events:				22621
■ Dilepton final state	Selection cuts			
	\mathcal{C}_1	\mathcal{C}_2	\mathcal{C}_3	\mathcal{C}_4
Signal benchmarks				
$M_{\phi_1} = 1250$ GeV, $M_{\nu_R} = 500$ GeV (pair production)	230	198	84	83
$M_{\phi_1} = 1250$ GeV, $M_{\nu_R} = 500$ GeV (single production)	304	249	112	107
Total number of dilepton signal events:				190
Background processes				
$Z_\ell (+2j)$	12438560	12006793	293294	6731
$t_\ell W_\ell (+2j)$	86150	82076	1055	148
$W_\ell Z_\ell (+2j)$	44839	43697	1304	186
$t_\ell t_\ell (+2j)$	253668	242057	3012	413
$W_\ell W_\ell (+2j)$	34671	33703	641	68
Total number of background events:				7546

TABLE III. Cut flow for two ϕ_1 benchmarks ($\lambda \rightarrow \{0, 1\}$) and the relevant background processes. The events are estimated for luminosity $\mathcal{L} = 3 \text{ ab}^{-1}$.

For backgrounds with very high cross sections, we apply some basic generational-level cuts to save computation time. For the dilepton final state, the $W_\ell + \text{jets}$ process can act as a background since a jet can be misidentified as a lepton. In fact, it is one of the major backgrounds for the RHN searches in with same-sign dilepton final states. Since we consider only opposite-sign lepton pairs, in our case, its contribution is not important as the jet-faking-lepton effi-

ciency is very small, $\sim 10^{-4}$ [53].

We show the cuts we apply on the two signals and the relevant backgrounds in Table II. In Table III, we show how these cuts affect various background processes. As examples, we also show the effect of the cuts on the signals for two ϕ_1 benchmarks.

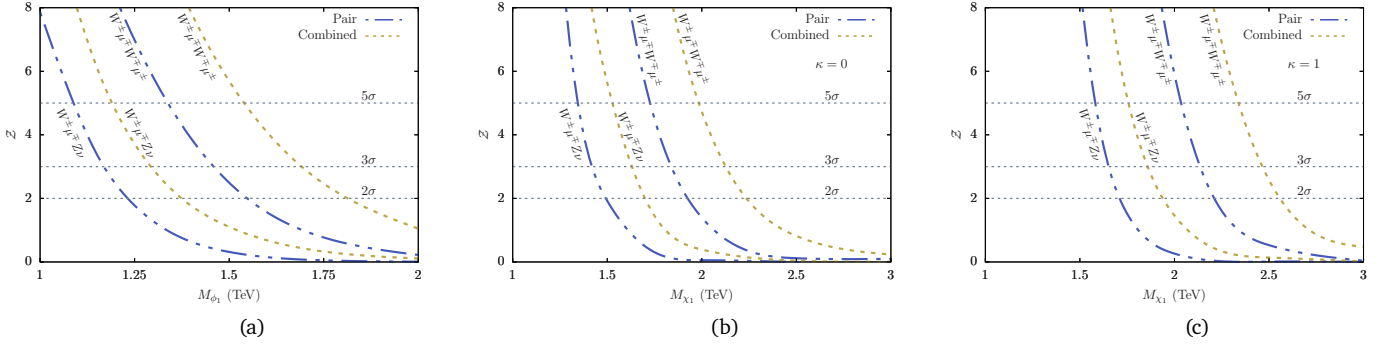


FIG. 2. Projected significance \mathcal{L} [Eq. (18)] of the (a) ϕ_1 and (b)-(c) χ_1 signals over the SM backgrounds for 3 ab^{-1} of integrated luminosity at the 14 TeV HL-LHC. Pair indicates only pair production contribution ($\lambda, \Lambda \rightarrow 0$), whereas the Combined ones are from the pair and single production processes. We have considered $\lambda, \Lambda = 1$ while computing the single production processes. We set $M_{V_R} = 500 \text{ GeV}$ in these plots.

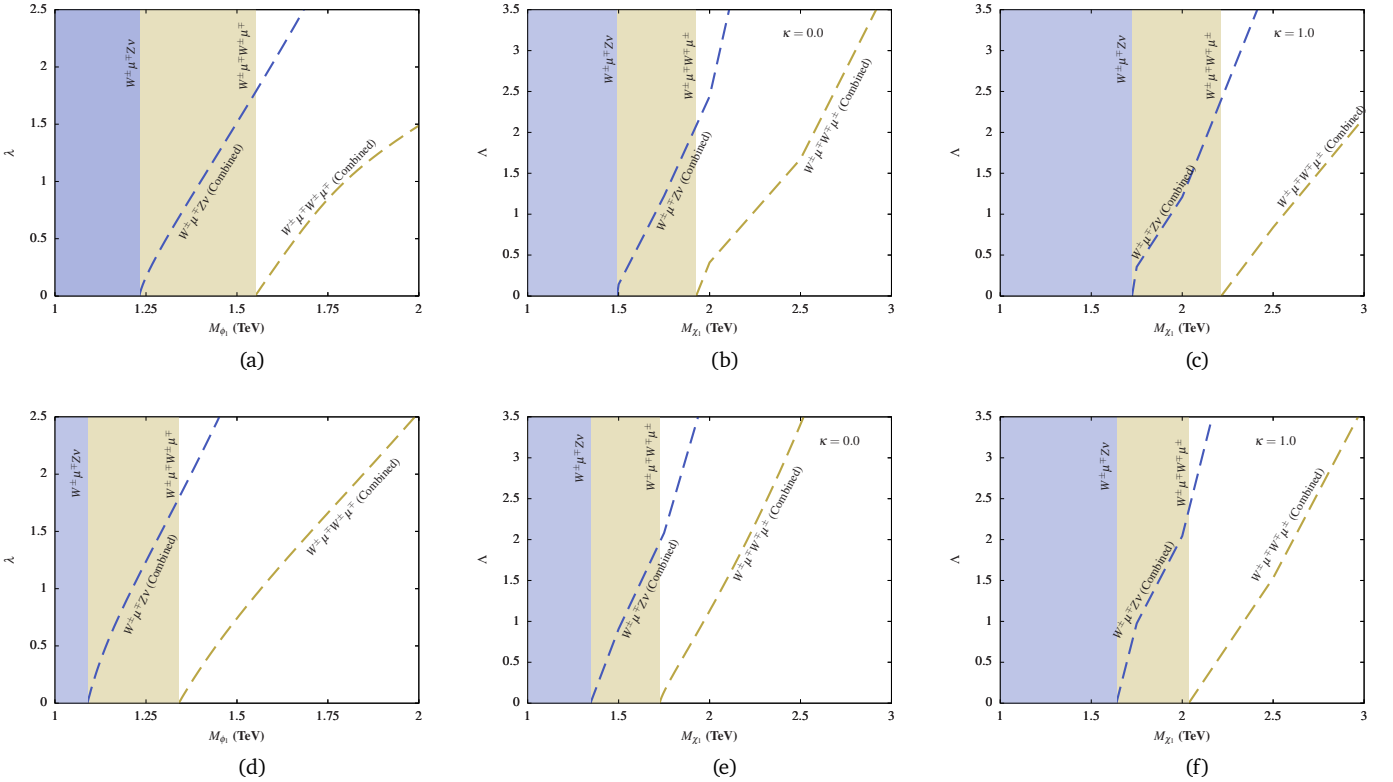


FIG. 3. The least values of the new couplings needed to observe the signals with 2σ [(a)-(c)] and 5σ [(d)-(f)] significances as functions of masses at the HL-LHC. The pair-production-only ($\lambda, \Lambda \rightarrow 0$) regions in the mono-lepton and dilepton channels are shown with solid colours. These plots are generated for $M_{V_R} = 500 \text{ GeV}$.

V. HL-LHC PROSPECTS

We use the following formula to compute the signal significance \mathcal{L} :

$$\mathcal{L} = \sqrt{2(N_S + N_B) \ln \left(\frac{N_S + N_B}{N_B} \right) - 2N_S}. \quad (18)$$

Here, N_S and N_B are the numbers of signal and background events surviving the selection cuts mentioned in Table II, respectively. We show \mathcal{L} as functions of the LQ masses

in Fig. 2. We see that the dilepton channel has better prospects. This is mainly because the branching ratio (BR) of the RHN in the $W\mu$ mode is roughly twice that of the ZV mode, i.e., $\text{BR}(v_R \rightarrow W^\pm \mu^\mp) \approx 2 \text{ BR}(v_R \rightarrow ZV)$, and the dilepton cuts perform relatively better due to higher μ -detection efficiency. In the dilepton channel, the 5σ discovery reach for ϕ_1 in the pair production mode can go as high as 1.3 TeV for $M_{V_R} = 500 \text{ GeV}$. But once the single production contributions (for $\lambda = 1$) are combined in the signal, the reach enhances to 1.5 TeV. Similarly, for χ_1 , the 5σ

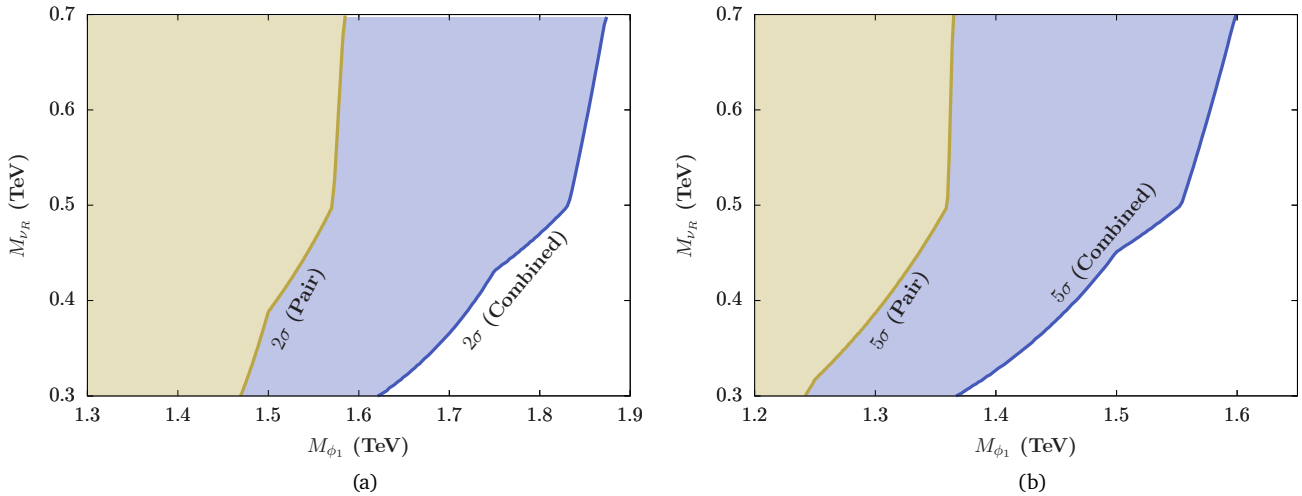


FIG. 4. The (a) 2σ and (b) 5σ contours in the dilepton mode on the M_{ϕ_1} - M_{ν_R} plane. The Combined contours are obtained for $\lambda = 1$.

reach in the pair-only mode is about 1.73 (2.04) GeV for the same RHN mass when $\kappa = 0$ ($\kappa = 1$), which increases to 1.98 (2.34) TeV when the single production events are combined in the signal. In the absence of discovery, the 2σ values show rough estimates of exclusion limits. For $M_{\nu_R} = 500$ GeV, the HL-LHC can exclude up to 1.81 TeV in the case of the ϕ_1 in the combined mode. The exclusion limits for χ_1 with $\kappa = 0$ and $\kappa = 1$ in the combined mode are 2.24 TeV and 2.56 TeV, respectively.

We project the 5σ and 2σ contours on the λ/Λ - M_{ϕ_1}/χ_1 planes in Fig. 3. These plots show the least values of the couplings necessary to obtain $\mathcal{Z} = 2$ or 5 with increasing LQ masses for $M_{\nu_R} = 500$ GeV. To understand how the signal significance varies with M_{ν_R} , we draw the 2σ and 5σ contours on the M_{ϕ_1} - M_{ν_R} plane in Fig. 4. We observe a drop in the sensitivity in the $M_{\nu_R} \ll M_{LQ}$ region. If the $M_{LQ} - M_{\nu_R}$ mass gap is large, the RHN becomes highly boosted, and the decay products of RHN become very collimated, making it difficult to isolate the W -like fatjet from the selected

muon. This requires a different strategy, as discussed in Ref. [54].

VI. CONCLUSIONS

In this paper, we have analysed the pair production of RHNs through LQ decays at the LHC. We have considered all possible scalar and vector LQs that can exclusively couple to RHNs and second-generation quarks. At the LHC, the LQs are produced either in pairs or singly, further producing a pair of RHNs in both cases. The RHNs decay to either a W boson and a muon or a Z/H boson and a neutrino, producing di and mono-lepton final states. We have analysed the prospects of these channels at the HL-LHC and obtained the 5σ and 2σ significance contours for a broad range of parameters.

-
- [1] P. Minkowski, $\mu \rightarrow e\gamma$ at a Rate of One Out of 10^9 Muon Decays?, *Phys. Lett. B* **67** (1977) 421–428.
 - [2] R. N. Mohapatra and G. Senjanovic, Neutrino Mass and Spontaneous Parity Nonconservation, *Phys. Rev. Lett.* **44** (1980) 912.
 - [3] R. N. Mohapatra, Mechanism for Understanding Small Neutrino Mass in Superstring Theories, *Phys. Rev. Lett.* **56** (1986) 561–563.
 - [4] R. N. Mohapatra and J. W. F. Valle, Neutrino Mass and Baryon Number Nonconservation in Superstring Models, *Phys. Rev. D* **34** (1986) 1642.
 - [5] S. Banerjee, P. S. B. Dev, A. Ibarra, T. Mandal and M. Mitra, Prospects of Heavy Neutrino Searches at Future Lepton Colliders, *Phys. Rev. D* **92** (2015) 075002, [1503.05491].
 - [6] W.-Y. Keung and G. Senjanovic, Majorana Neutrinos and the Production of the Right-handed Charged Gauge Boson, *Phys. Rev. Lett.* **50** (1983) 1427.
 - [7] M. Thomas Arun, T. Mandal, S. Mitra, A. Mukherjee, L. Priya and A. Sampath, Testing left-right symmetry with an inverse seesaw mechanism at the LHC, *Phys. Rev. D* **105** (2022) 115007, [2109.09585].
 - [8] A. Ekstedt, R. Enberg, G. Ingelman, J. Löfgren and T. Mandal, Constraining minimal anomaly free U(1) extensions of the Standard Model, *JHEP* **11** (2016) 071, [1605.04855].
 - [9] D. Choudhury, K. Deka, T. Mandal and S. Sadhukhan, Neutrino and Z' phenomenology in an anomaly-free U(1) extension: role of higher-dimensional operators, *JHEP* **06** (2020) 111, [2002.02349].
 - [10] K. Deka, T. Mandal, A. Mukherjee and S. Sadhukhan, Leptogenesis in an anomaly-free U(1) extension with higher-dimensional operators, [2105.15088](#).
 - [11] M. T. Arun, A. Chatterjee, T. Mandal, S. Mitra, A. Mukherjee and K. Nivedita, Search for the Z' boson decaying to a right-handed neutrino pair in leptophobic U(1)

- models, *Phys. Rev. D* **106** (2022) 095035, [2204.02949].
- [12] J. C. Pati and A. Salam, *Lepton Number as the Fourth Color*, *Phys. Rev. D* **10** (1974) 275–289. [Erratum: Phys. Rev. D **11**, 703 (1975)].
- [13] H. Georgi and S. L. Glashow, *Unity of All Elementary Particle Forces*, *Phys. Rev. Lett.* **32** (1974) 438–441.
- [14] B. Schrempp and F. Schrempp, *Light Leptoquarks*, *Phys. Lett.* **B153** (1985) 101–107.
- [15] R. Barbier et al., *R-parity violating supersymmetry*, *Phys. Rept.* **420** (2005) 1–202, [hep-ph/0406039].
- [16] T. Mandal, S. Mitra and S. Raz, *$R_{D^{(*)}}$ motivated \mathcal{S}_1 leptoquark scenarios: Impact of interference on the exclusion limits from LHC data*, *Phys. Rev. D* **99** (2019) 055028, [1811.03561].
- [17] U. Aydemir, T. Mandal and S. Mitra, *Addressing the $R_{D^{(*)}}$ anomalies with an \mathbf{S}_1 leptoquark from $\mathbf{SO}(10)$ grand unification*, *Phys. Rev. D* **101** (2020) 015011, [1902.08108].
- [18] A. Bhaskar, D. Das, T. Mandal, S. Mitra and C. Neeraj, *Precise limits on the charge-2/3 U_1 vector leptoquark*, *Phys. Rev. D* **104** (2021) 035016, [2101.12069].
- [19] A. Bhaskar, A. A. Madathil, T. Mandal and S. Mitra, *Combined explanation of W -mass, muon $g-2$, $RK^{(*)}$ and $RD^{(*)}$ anomalies in a singlet-triplet scalar leptoquark model*, *Phys. Rev. D* **106** (2022) 115009, [2204.09031].
- [20] U. K. Dey, D. Kar, M. Mitra, M. Spannowsky and A. C. Vincent, *Searching for Leptoquarks at IceCube and the LHC*, *Phys. Rev. D* **98** (2018) 035014, [1709.02009].
- [21] P. Bandyopadhyay and R. Mandal, *Revisiting scalar leptoquark at the LHC*, *Eur. Phys. J. C* **78** (2018) 491, [1801.04253].
- [22] K. Chandak, T. Mandal and S. Mitra, *Hunting for scalar leptoquarks with boosted tops and light leptons*, *Phys. Rev. D* **100** (2019) 075019, [1907.11194].
- [23] R. Padhan, S. Mandal, M. Mitra and N. Sinha, *Signatures of \tilde{R}_2 class of Leptoquarks at the upcoming ep colliders*, *Phys. Rev. D* **101** (2020) 075037, [1912.07236].
- [24] A. Bhaskar, T. Mandal and S. Mitra, *Boosting vector leptoquark searches with boosted tops*, *Phys. Rev. D* **101** (2020) 115015, [2004.01096].
- [25] N. Ghosh, S. K. Rai and T. Samui, *Collider Signatures of a Scalar Leptoquark and Vector-like Lepton in Light of Muon Anomaly*, 2206.11718.
- [26] ATLAS collaboration, G. Aad et al., *Search for pairs of scalar leptoquarks decaying into quarks and electrons or muons in $\sqrt{s} = 13$ TeV pp collisions with the ATLAS detector*, *JHEP* **10** (2020) 112, [2006.05872].
- [27] ATLAS collaboration, *Search for pair-produced scalar and vector leptoquarks decaying into third-generation quarks and first- or second-generation leptons in pp collisions with the ATLAS detector*, 2210.04517.
- [28] D. Das, K. Ghosh, M. Mitra and S. Mondal, *Probing sterile neutrinos in the framework of inverse seesaw mechanism through leptoquark productions*, *Phys. Rev. D* **97** (2018) 015024, [1708.06206].
- [29] S. Mandal, M. Mitra and N. Sinha, *Probing leptoquarks and heavy neutrinos at the LHeC*, *Phys. Rev. D* **98** (2018) 095004, [1807.06455].
- [30] A. Bhaskar, D. Das, B. De and S. Mitra, *Enhancing scalar productions with leptoquarks at the LHC*, *Phys. Rev. D* **102** (2020) 035002, [2002.12571].
- [31] G. Cottin, O. Fischer, S. Mandal, M. Mitra and R. Padhan, *Displaced neutrino jets at the LHeC*, *JHEP* **06** (2022) 168, [2104.13578].
- [32] A. Bhaskar, D. Das, B. De, S. Mitra, A. K. Nayak and C. Neeraj, *Leptoquark-assisted singlet-mediated di-Higgs production at the LHC*, *Phys. Lett. B* **833** (2022) 137341, [2205.12210].
- [33] A. Bhaskar, T. Mandal, S. Mitra and M. Sharma, *Improving third-generation leptoquark searches with combined signals and boosted top quarks*, *Phys. Rev. D* **104** (2021) 075037, [2106.07605].
- [34] I. Doršner, S. Fajfer, A. Greljo, J. F. Kamenik and N. Košnik, *Physics of leptoquarks in precision experiments and at particle colliders*, *Phys. Rept.* **641** (2016) 1–68, [1603.04993].
- [35] A. Alloul, N. D. Christensen, C. Degrande, C. Duhr and B. Fuks, *FeynRules 2.0 - A complete toolbox for tree-level phenomenology*, *Comput. Phys. Commun.* **185** (2014) 2250–2300, [1310.1921].
- [36] C. Degrande, C. Duhr, B. Fuks, D. Grellscheid, O. Mattelaer and T. Reiter, *UFO - The Universal FeynRules Output*, *Comput. Phys. Commun.* **183** (2012) 1201–1214, [1108.2040].
- [37] J. Alwall, R. Frederix, S. Frixione, V. Hirschi, F. Maltoni, O. Mattelaer et al., *The automated computation of tree-level and next-to-leading order differential cross sections, and their matching to parton shower simulations*, *JHEP* **07** (2014) 079, [1405.0301].
- [38] M. Kramer, T. Plehn, M. Spira and P. M. Zerwas, *Pair production of scalar leptoquarks at the CERN LHC*, *Phys. Rev. D* **71** (2005) 057503, [hep-ph/0411038].
- [39] T. Mandal, S. Mitra and S. Seth, *Pair Production of Scalar Leptoquarks at the LHC to NLO Parton Shower Accuracy*, *Phys. Rev. D* **93** (2016) 035018, [1506.07369].
- [40] T. Sjöstrand, S. Ask, J. R. Christiansen, R. Corke, N. Desai, P. Ilten et al., *An introduction to PYTHIA 8.2*, *Comput. Phys. Commun.* **191** (2015) 159–177, [1410.3012].
- [41] DELPHES 3 collaboration, J. de Favereau, C. Delaere, P. Demin, A. Giammanco, V. Lemaître, A. Mertens et al., *DELPHES 3, A modular framework for fast simulation of a generic collider experiment*, *JHEP* **02** (2014) 057, [1307.6346].
- [42] M. Cacciari, G. P. Salam and G. Soyez, *The anti- k_r jet clustering algorithm*, *JHEP* **04** (2008) 063, [0802.1189].
- [43] M. Cacciari, G. P. Salam and G. Soyez, *FastJet User Manual*, *Eur. Phys. J. C* **72** (2012) 1896, [1111.6097].
- [44] T. Mandal and S. Mitra, *Probing Color Octet Electrons at the LHC*, *Phys. Rev. D* **87** (2013) 095008, [1211.6394].
- [45] T. Mandal, S. Mitra and S. Seth, *Single Productions of Colored Particles at the LHC: An Example with Scalar Leptoquarks*, *JHEP* **07** (2015) 028, [1503.04689].
- [46] T. Mandal, S. Mitra and S. Seth, *Probing Compositeness with the CMS $eejj$ & eej Data*, *Phys. Lett. B* **758** (2016) 219–225, [1602.01273].
- [47] S. Catani, L. Cieri, G. Ferrera, D. de Florian and M. Grazzini, *Vector boson production at hadron colliders: a fully exclusive QCD calculation at NNLO*, *Phys. Rev. Lett.* **103** (2009) 082001, [0903.2120].
- [48] G. Balossini, G. Montagna, C. M. Carloni Calame, M. Moretti, O. Nicrosini, F. Piccinini et al., *Combination of electroweak and QCD corrections to single W production at the Fermilab Tevatron and the CERN LHC*, *JHEP* **01** (2010) 013, [0907.0276].
- [49] J. M. Campbell, R. K. Ellis and C. Williams, *Vector boson pair production at the LHC*, *JHEP* **07** (2011) 018, [1105.0020].
- [50] N. Kidonakis, *Theoretical results for electroweak-boson and single-top production*, *PoS DIS2015* (2015) 170, [1506.04072].
- [51] C. Muselli, M. Bonvini, S. Forte, S. Marzani and G. Ridolfi, *Top Quark Pair Production beyond NNLO*, *JHEP* **08** (2015)

- 076, [1505.02006].
- [52] A. Kulesza, L. Motyka, D. Schwartländer, T. Stebel and V. Theeuwes, *Associated production of a top quark pair with a heavy electroweak gauge boson at NLO+NNLL accuracy*, *Eur. Phys. J. C* **79** (2019) 249, [1812.08622].
- [53] D. Curtin, J. Galloway and J. G. Wacker, *Measuring the $t\bar{t}h$ coupling from same-sign dilepton $+2b$ measurements*, *Phys. Rev. D* **88** (2013) 093006, [1306.5695].
- [54] M. Mitra, R. Ruiz, D. J. Scott and M. Spannowsky, *Neutrino Jets from High-Mass W_R Gauge Bosons in TeV-Scale Left-Right Symmetric Models*, *Phys. Rev. D* **94** (2016) 095016, [1607.03504].